HAL
open science

# Cyclobishelicenes: shape-persistent figure-eight aromatic molecules with promising chiroptical properties

Antoine Robert, Guillaume Naulet, Harald Bock, Nicolas Vanthuyne, Marion Jean, Michel Giorgi, Yannick Carissan, Christie Aroulanda, Antoine Scalabre, Emilie Pouget, et al.

## ▶ To cite this version:

Antoine Robert, Guillaume Naulet, Harald Bock, Nicolas Vanthuyne, Marion Jean, et al.. Cyclobishelicenes: shape-persistent figure-eight aromatic molecules with promising chiroptical properties. Chemistry - A European Journal, 2019, 25 (63), pp.14364-14369. 10.1002/chem.201902637 . hal-02265747

**HAL Id: hal-02265747**

**https://amu.hal.science/hal-02265747**

Submitted on 24 Oct 2019

**HAL** is a multi-disciplinary open access archive for the deposit and dissemination of scientific research documents, whether they are published or not. The documents may come from teaching and research institutions in France or abroad, or from public or private research centers.

L'archive ouverte pluridisciplinaire **HAL**, est destinée au dépôt et à la diffusion de documents scientifiques de niveau recherche, publiés ou non, émanant des établissements d'enseignement et de recherche français ou étrangers, des laboratoires publics ou privés.

# Cyclobishelicenes: Shape-Persistent Figure-Eight Aromatic Molecules with Promising Chiroptical Properties

Antoine Robert,[a] Guillaume Naulet,[a] Harald Bock,[a] Nicolas Vanthuyne,[b] Marion Jean,[b] Michel Giorgi,[c] Yannick Carissan,[b] Christie Aroulanda,[d] Antoine Scalabre,[e] Emilie Pouget,[e] Fabien Durola,*[a] and Yoann Coquerel*[b]

**Abstract:** Cyclobis[*n*]helicenes ($n = 3$ or 5) are chiral $D_2$-symmetric π-conjugated macrocycles with stable lemniscular, or figure-eight, shapes. The conformational analysis of five different cyclobis[*n*]helicenes revealed that these molecules can only exist as their lemniscular conformers with high barriers to enantiomerization (> 200 kJ mol$^{-1}$). The enantiomers of a cyclobis[5]helicene were resolved by HPLC and their unusual chiroptical properties were attributed to the inherent chirality of their macrocyclic figure-eight.

## Introduction

Molecular chirality is a property of utmost importance in chemical and physical sciences, as well as in medicine and technology.[1] Chiral shape-persistent π-conjugated macrocycles are molecules of enormous fundamental interest, at this stage, and are extremely rare.[2] Cyclobis[*n*]helicenes appear as perfect prototypes of chiral and configurationally stable macrocycles with lemniscular, that is figure-eight, shapes having $D_2$ symmetry, and no data is currently available on the chirality-related properties of these molecules (Figure 1). Cyclobisphenanthrene or dibenzo[*def*,*pqr*]tetraphenylene (**1 a**), a negatively curved cyclooctatetraene derivative that may be regarded as a cyclobis[3]helicene considering the severe helical distortion of its two phenanthrene units, was synthesized as early as 1977 by Thulin and Wennerström who concluded that this molecule must be considerably twisted and of $D_2$ symmetry, with a barrier to enantiomerization higher than 108.7 kJ mol$^{-1}$.[3] Sheldrick reported the X-ray structure of **1 a** in 1981 with both enantio-

[a] *Dr. A. Robert, Dr. G. Naulet, Dr. H. Bock, Dr. F. Durola*
*Centre de Recherche Paul Pascal, CNRS, Bordeaux Univ*
*115 av. Schweitzer, 33600 Pessac (France)*
*E-mail: fabien.durola@crpp.cnrs.fr*

[b] *Dr. N. Vanthuyne, M. Jean, Dr. Y. Carissan, Dr. Y. Coquerel*
*Aix Marseille Univ, CNRS, Centrale Marseille, ISM2, 13397 Marseille (France)*
*E-mail: yoann.coquerel@univ-amu.fr*

[c] *Dr. M. Giorgi*
*Aix Marseille Univ, CNRS, Centrale Marseille, FSCM, Marseille (France)*

[d] *Dr. C. Aroulanda*
*ERMN, ICMMO, UMR CNRS 8182, Paris-Sud, Paris Saclay Univ., Orsay (France)*

[e] *A. Scalabre, Dr. E. Pouget*
*Chimie et Biologie des Membranes et des Nanoobjets (CBMN)*
*CNRS, Bordeaux Univ, Bordeaux INP, UMR5248*
*Allée St Hilaire, Bat B14, 33607 Pessac (France)*

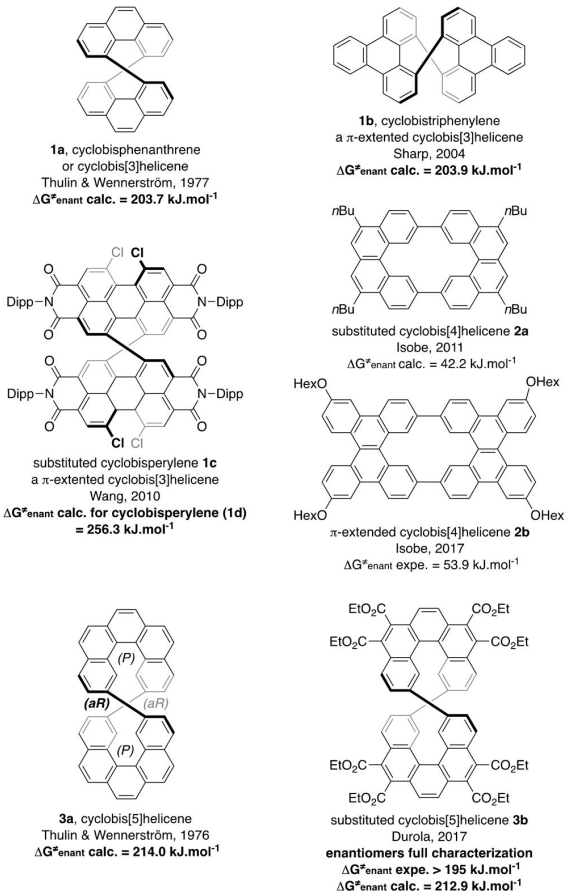


**Figure 1.** Known cyclobis[*n*]helicenes and scope of the present study (in bold).

mers embedded in the crystal and confirmed the assumptions of Thulin and Wennerström on its geometry.[4] π-Extended analogs of cyclobisphenanthrene (**1 a**) were prepared more recently, namely cyclobistriphenylene (**1 b**)[5] and the functionalized cyclobisperylene **1 c**.[6] Significantly, the enantiomers of **1 c** have been resolved by HPLC and found configurationally stable for three hours at 150 °C and their absolute configurations were tentatively assigned without further investigation. The substituted cyclobis[4]helicenes **2 a**,**b** were reported by Isobe.[7] These molecules can adopt several moderately distorted conformations that interconvert rapidly at 20 °C with barriers to enantiomerization determined at 42.2 and 53.9 kJ mol$^{-1}$, respectively. Their time-averaged structures may actually be regarded as flat planes without peculiar topology. Cyclobis[5]helicene (**3 a**) was synthesized, again, by Thulin and Wennerström in the early days of chiral polycyclic aromatic hydrocarbons chemistry and its fluorescence properties examined.[8] Recently, the synthesis of the substituted octaester analog **3 b** was reported by some of us.[9]

Herein, we report the resolution of cyclobis[5]helicene **3 b** by HPLC techniques, and the full structural, chiroptical, and conformational analyses of its enantiomers. The computed enantiomerization processes and barriers to enantiomerization of all cyclobis[*n*]helicenes in Figure 1 are also reported.

## Results and Discussion

Unsubstituted cyclobis[*n*]helicenes contain four individual stereogenic elements: two [*n*]helicenes with helical chirality and two biaryl units with axial chirality. They could thus theoretically exist as four distinct conformers, each forming a pair of enantiomers: a $D_2$-symmetric figure-eight-shaped conformer, two $C_2$-symmetric conformers and one $C_1$-symmetric conformer. The figure-eight conformers depicted in Figure 1 having (*P*)-configured helicenes combined with (*aR*)-configured axes offer the optimum spatial arrangements. While all metastable conformers may transiently exist for cyclobis[4]helicenes,[7b] geometrical constraints limit the flexibility of cyclobis[3]helicenes and cyclobis[5]helicenes (see below).

Cyclobis[5]helicene **3 b** was prepared in the racemic series as previously described[9] by using a glyoxylic Perkin reaction for the formation of the intermediate flexible macrocycle **4**, which was rigidified by a four-fold Mallory photocyclization (Scheme 1). Racemic [5]helicene **6** was prepared by the same approach.[10]

The discrimination of the enantiomers of **3 b** was first investigated by using NMR spectroscopy in chiral liquid crystals.[11] Indeed, because of enantioselective solute–solvent interactions in those mesophases, enantiomers orient themselves differently, which leads to different NMR observables such as, for instance, $^{13}$C chemical shifts because of different $^{13}$C chemical shift anisotropy terms. In practice, three $^{13}$C-{$^1$H} NMR spectra of racemic **3 b** were recorded in (a) $CD_2Cl_2$ alone, (b) a chiral liquid crystalline solvent made of a chiral enantiopure polymer, poly-γ-benzyl-*L*-glutamate (PBLG) dissolved in $CD_2Cl_2$, and c) a racemic liquid crystalline solvent made of a 1:1 PBLG and its enantiomer PBDG dissolved in $CD_2Cl_2$ as a control experiment

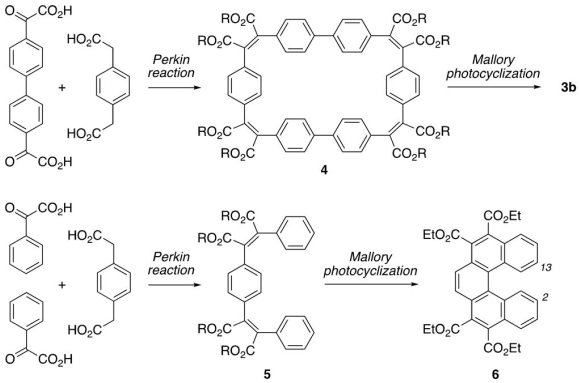


**Scheme 1.** Highlights of the syntheses of cyclobis[5]helicene **3 b** and [5]helicene **6**.

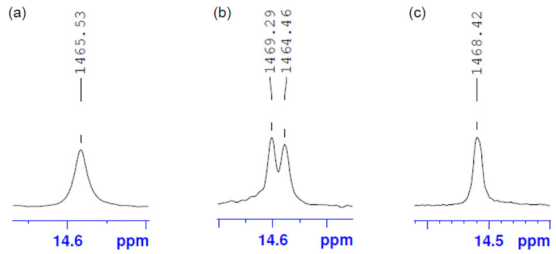


**Figure 2.** 100 MHz $^{13}$C-{$^1$H} NMR spectra (in part) of racemic **3 b** in a) $CD_2Cl_2$ alone, b) a chiral liquid crystalline solvent PBLG/$CD_2Cl_2$, and c) a racemic liquid crystalline solvent made of 1:1 PBLG:PBDG/$CD_2Cl_2$. Peak picking is reported in [Hz], see the Supporting Information for full details.

(Figure 2). Spectral enantiodifferentiation of the two enantiomers was observed on various sites on the molecule when data were recorded in the enantiopure mesophase, as illustrated in Figure 2 for the methyl groups of the ethyl esters ($\delta \approx 14.5$ ppm, see also the Supporting Information).

The resolution of **3 b** was achieved by semipreparative HPLC methods (see the Supporting Information), and both enantiomers were obtained as enantiopure materials (first eluted: >99 % *ee*, second eluted: >98 % *ee*). Structurally, cyclobis[5]helicene **3 b** may be regarded as a cyclodimer of the substituted [5]helicene **6**, the C2 and C13 atoms of which are linked in a head-to-tail manner, and the enantiomers of **6** were also resolved. The absolute configurations of the enantiomers of **3 b** and **6** were safely determined from their structural and chiroptical analyses (see below and the Supporting Information). The structure of crystalline racemic **3 b** was previously resolved by X-ray diffraction techniques,[9a] and for the present work the structures of both enantiomers of **3 b** were determined, which allowed unambiguous assignment of their respective absolute configurations (Figure 3).[12] The first eluted enantiomer of **3 b** was found (*P*,*aR*,*P*,*aR*)-configured and the second eluted enantiomer was, logically, confirmed as (*M*,*aS*,*M*,*aS*)-configured. These assignments were also confirmed by circular dichroism spectroscopy (see below).

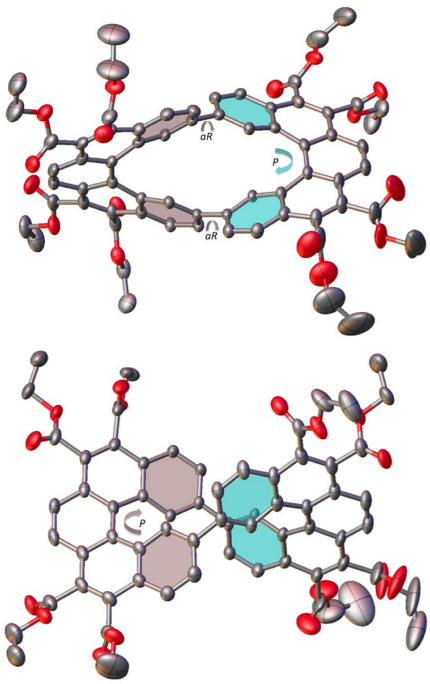


**Figure 3.** Representation of the structure of (*P,aR,P,aR*)-**3 b** obtained by X-ray diffraction analyses. Top: top view; bottom: side view. Representative interplanar angles and torsion angles are highlighted. Only one molecule of the asymmetric unit has been drawn and H atoms and solvent molecules have been omitted for clarity.

The racemic and enantiopure crystals obviously have different packings and supramolecular arrangements in the solid state, and their molecular structural parameters were found very similar in the three structures. As previously analyzed from racemic **3 b**, the [5]helicene fragments in enantiopure **3 b** are nearly undistorted compared with [5]helicene itself. For instance, the interplanar angles between the two terminal rings of each [5]helicene unit range from 35.90 to 39.21° in the racemic crystal, and from 37.79 to 41.62° in the enantiopure crystals (Figure 3). In comparison, the interplanar angle in [5]helicene itself is 46.0°.[13] Similarly, the mean torsion angles at the stereogenic axes range from 59.64 to 65.06° in the racemate and from 60.80 to 65.29° in the enantiopure crystals, which indicates no unusual strain around the stereogenic axes. The average lengths of the single $C_{sp^2}$–$C_{sp^2}$ bonds linking the two [5]helicene units were found nearly identical in the three structures, ranging from 1.449 to 1.515 Å, which corresponds to the lengths observed in biphenyls.[14] These new measurements confirmed that the figure-eight macrocyclic conformational arrangement in **3 b** nicely accommodates its four individual stereogenic elements with an overall very moderate strain. At the supramolecular level, intermolecular interactions and solvent (chloroform) distribution are somewhat different within the crystals made of racemic and enantiopure **3 b**. While solvent voids represent less than 7% of the cell volume and build up continuous channels along the cell axis *a* in the racemate, they account for about 12% of the cell volume and are distributed as separate pockets along the unit cell axis *a* in the enantiopure crystals. Accordingly, crystalline enantiopure **3 b** appears less dense than the racemic material, which is consistent with the analysis of the intermolecular interactions in both materials. Only two significant π–π interactions ($\alpha \leq 16°$, slippage ≤ 1.5 Å and Cg–Cg ≤ 4.0 Å; α: dihedral angle between the two rings, slippage: distance between the centroid of one ring to the perpendicular projection of the second ring, Cg–Cg: distance between the centroids Cg of the two rings) could be found in the enantiopure crystals of **3 b** and therefore are only observed within the asymmetric unit. In contrast, eight significant π–π interactions were found in the racemic crystal that apply to molecules within the asymmetric unit as well as symmetry-related molecules within the crystal. Similarly, a single CH–π interaction was found in crystalline enantiopure **3 b** and nine of them were identified in the racemate.

The chiroptical properties of cyclobis[5]helicene **3 b** were examined and compared with those of the [5]helicene **6**. The optical rotations of enantiopure **3 b** and **6** were measured in dichloromethane at four different wavelengths (Table 1). Strikingly, the sign of the optical rotation of the cyclobis[5]helicene (*P,aR,P,aR*)-**3 b** was the opposite of the one of the [5]helicene (*P*)-**6** by a large magnitude, and of course the same holds for (*M,aS,M,aS*)-**3 b** relative to (*M*)-**6**. This is largely unexpected because (*P*)-configured helicenes invariably lead to positive $[\alpha]_D^{25}$ values.[15]

**Table 1.** Optical rotations of enantiopure **3 b** and **6** (R = $CO_2Et$).

| λ (nm) | $[\alpha]_\lambda^{25}$ 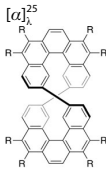 (*P,aR,P,aR*)-**3b** | $[\alpha]_\lambda^{25}$ (*M,aS,M,aS*)-**3b** | $[\alpha]_\lambda^{25}$ 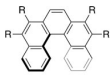 (*P*)-**6** | $[\alpha]_\lambda^{25}$ 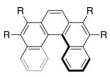 (*M*)-**6** |
|---|---|---|---|---|
| 589 | −1000 | +1000 | +680 | −680 |
| 578 | −1050 | +1050 | +720 | −720 |
| 546 | −1400 | +1400 | +890 | −890 |
| 436 | −7500 | +7500 | +2100 | −2100 |

The comparison of the experimental and simulated UV/Vis and electronic circular dichroism (ECD) spectra of the cyclobis[5]helicene (*P,aR,P,aR*)-**3 b** and the [5]helicene (*P*)-**6** was also informative. The superimposition of the spectra is presented in Figure 4 with those of (*P*)-**6** scaled by a factor 2 on the absorbance axis for direct comparison. The experimental spectra recorded for (*P,aR,P,aR*)-**3 b** and (*P*)-**6** are barely comparable. The UV/Vis spectrum of (*P,aR,P,aR*)-**3 b** is globally redshifted relative to the one of (*P*)-**6**. The ECD spectrum of (*P,aR,P,aR*)-**3 b** differed dramatically from the one of (*P*)-**6**. Most significantly, the bands are inversed between 185 and 250 nm, and the cyclobis[5]helicene (*P,aR,P,aR*)-**3 b** shows an intense band between 350 and 400 nm, whereas there is almost no signal in this region for the [5]helicene (*P*)-**6**. However, the ECD spectra are

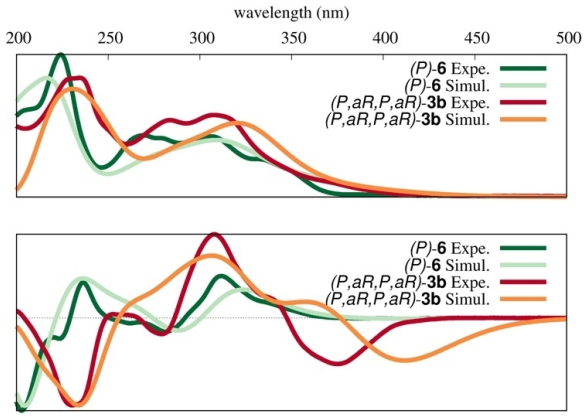


**Figure 4.** Superimposition of the experimental and simulated UV/Vis (top) and ECD (bottom) spectra of (*P*)-**6**, scaled by a factor 2 on the vertical absorbance axis for the latter, and (*P,aR,P,aR*)-**3 b**. TD-DFT calculations were performed at the PBE0/def2-SV(P) level of theory with the random phase approximation approach.

more or less comparable in the 250–350 nm region, a marker of the carbohelicenes.[15] Simulations of the UV/Vis and ECD spectra of (*P,aR,P,aR*)-**3 b** and (*P*)-**6** were performed by using DFT methods (see the Supporting Information for details). The computed spectra fairly matched the experimental spectra, however, with a notable difference: the band observed experimentally at 350–400 nm in the ECD spectrum of (*P,aR,P,aR*)-**3 b** is redshifted by about 50 nm in the simulation. The circularly polarized luminescence (CPL) response of (*P,aR,P,aR*)-**3 b** and (*M,aS,M,aS*)-**3 b** was also investigated. As expected, strong CPL with opposite signals can be observed around the fluorescence emission (Figure 5). CPL characteristics of a molecule are quantified by the luminescence dissymmetry factor $g_{lum}$. The value $|g_{lum}| = 5.10^{-3}$ measured for **3 b** at the maximum of fluorescence (447 nm) is in the high of the range of values for organic molecules (comparatively, $|g_{lum}| = 0.14.10^{-3}$ for [6]helicene).[16] Overall, the chiroptical properties of the cyclobis[5]helicene **3 b** are not governed by the chirality of its two homochiral [5]helicene units but seemingly by the inherent chirality of its macrocyclic figure-eight.[2]

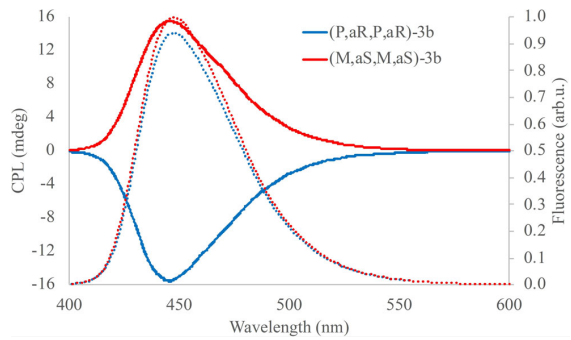


**Figure 5.** Circularly polarized luminescence (CPL) spectra of (*P,aR,P,aR*)-**3 b** (blue) and (*M,aS,M,aS*)-**3 b** (red). The dashed lines are the fluorescence emissions. Concentration = 8 μmol L$^{-1}$ in dichloromethane. The excitation wavelength was 315 nm.

No data is currently available on the conformational behavior and configurational stability of cyclobis[3]helicenes and cyclobis[5]helicenes. For the present work, we have computationally investigated the flexibility of cyclobis[5]helicenes **3 a** and **3 b** and computed their barriers to enantiomerization (Figure 6). A similar study for cyclobis[3]helicenes **1 a**, **1 b**, and

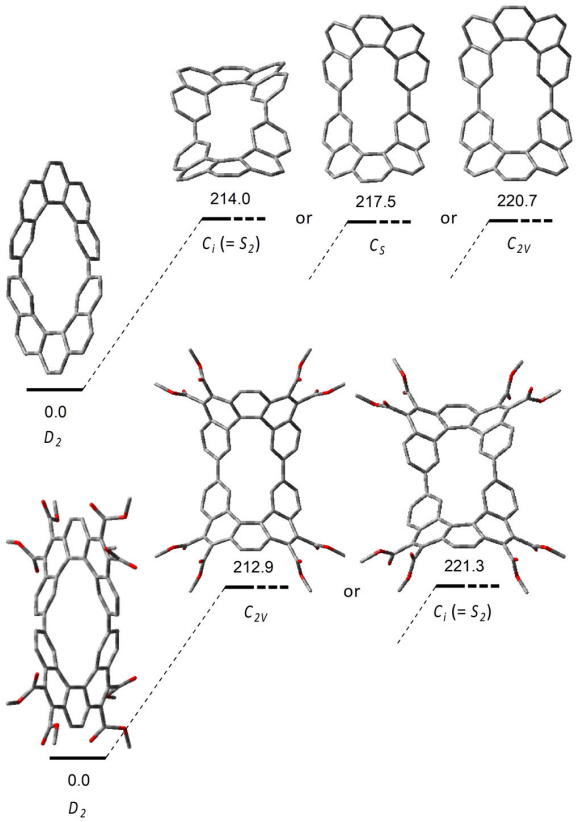


**Figure 6.** Enantiomerization processes of the cyclobis[5]helicenes **3 a** (top) and **3 b**$_{Me}$ (bottom) obtained by DFT calculations, see the Supporting Information for details. Symmetry groups are noted below each stationary point, H atoms are omitted for clarity, and Gibbs free energies are reported in [kJ mol$^{-1}$].

**1 d** is available in the Supporting Information. The DFT calculations were performed by using PBE0-D3/def2-TZVP//PBE0-D3/6-31G(d), a level of theory recently demonstrated suitable for large [*n*]helicenes.[17] Cyclobis[5]helicene (**3 a**) inverted its absolute configuration preferentially through a single centrosymmetric transition state computed at $\Delta G^{\neq}_{enant} = 214.0$ kJ mol$^{-1}$ (Figure 6, top). Two single-step alternative paths involving nearly isoenergetic transition states with $C_s$ and $C_{2v}$ symmetry, computed at $\Delta G^{\neq}_{enant} = 217.5$ kJ mol$^{-1}$ and $\Delta G^{\neq}_{enant} = 220.7$ kJ mol$^{-1}$, respectively, were also located. Relative errors greater than ± 10 kJ mol$^{-1}$ are certainly possible in the computational model. It is remarkable that both [5]helicenes and

both stereogenic axes in **3a** inverse their configurations in a single event, whatever the path followed. This was attributed to geometrical factors inherent to the [5]helicene moieties and their head-to-tail connectivity by their C2 and C13 atoms. Similarly, two roughly isoenergetic single-step enantiomerization paths were found for cyclobis[5]helicene $\mathbf{3b_{Me}}$, the methyl ester analog of **3b** employed for the calculations: a $C_{2v}$-symmetric transition state calculated at $\Delta G^{\neq}_{enant} = 212.9\ kJ\,mol^{-1}$ and a centrosymmetric transition state calculated slightly higher in energy at $\Delta G^{\neq}_{enant} = 221.3\ kJ\,mol^{-1}$ (Figure 6, bottom). Notably, the presence of the ester substituents induced a relative stabilization of the $C_{2v}$-symmetric transition state. While we could easily determine experimentally the barrier to enantiomerization of the [5]helicene **6** to be $\Delta G^{\neq}_{enant} = 104.3\ kJ\,mol^{-1}$, which compared nicely with its computed value $\Delta G^{\neq}_{enant} = 104.7\ kJ\,mol^{-1}$, heating a 1,2,4-trichlorobenzene solution of enantiopure (*P,aR,P,aR*)-**3b** (*ee* $>99\%$) at 214 °C for 16 days resulted in no detectable loss of the enantiomeric purity or degradation. This confirmed the high thermal stability of **3b** and indicated a high barrier to enantiomerization greater than 195 $kJ\,mol^{-1}$ in line with the calculations and practically difficult to measure experimentally. Generally, it was found that cyclobis[3]helicenes enantiomerize through transition states or high-energy metastable intermediates with $C_{2h}$ symmetry (see the Supporting Information), whereas the enantiomerization of cyclobis[5]helicenes preferentially proceeds via $C_i$- or $C_{2v}$-symmetric transition states. Overall, the lemniscular shapes of cyclobis[3]helicenes and cyclobis[5]helicenes are responsible for their high configurational stability and their unusual single-step, or just like, enantiomerization processes.

Some double, triple, and hextuple [5]helicenes with $D_n$ symmetry have been prepared in the past few years as chiral propeller-shaped nanographenes (Figure 7).[18] The enantiomerization processes of these multiple helicenes involve multiple transition states (one per [5]helicene unit in the structure) and their barriers are in the range $\Delta G^{\neq}_{enant} = 109.9–152.8\ kJ\,mol^{-1}$, which indicates that they are much more flexible and prone to racemization than cyclobis[5]helicenes **3a** and **3b**. Also, the global chiroptical properties of the multiple helicenes in Figure 7 can be roughly estimated as the sum of the individual chiroptical properties of each [5]helicene unit in the structure, which is not the case for cyclobis[5]helicene **3b** (see Table 1 and Figures 4 and 5). In a broader meaning, we suggest that multiple helicenes on the one hand and cyclohelicenes on the other hand should be regarded as two distinct classes of helicene-containing chiral polycyclic aromatic hydrocarbons.

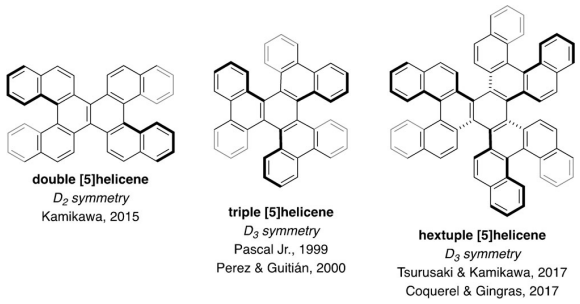


**Figure 7.** Previously synthesized multiple [5]helicenes with $D_n$ symmetry.

## Conclusions

In summary, the conformational behavior and enantiomerization processes of cyclobis[3]helicenes and cyclobis[5]helicenes were investigated, together with the chiroptical properties of a cyclobis[5]helicene. It was found that these molecules are exceptionally conformationally stable for medium-sized rings and macrocycles with very rigid but yet moderately strained conformations, and barriers to enantiomerization greater than 200 $kJ\,mol^{-1}$. The chiroptical responses of cyclobis[5]helicene **3b** were of large magnitude, for instance with $|[\alpha]^{25}_{D}| = 1000$, and not directly correlated with the chiroptical properties of [5]helicene **6**. The inherent chirality of the macrocyclic figure-eight is apparently responsible for these remarkable chiroptical properties. Cyclobis[5]helicene **3b** is a very rare example of a polyaromatic molecule embedding a stable lemniscular conformation allowing for its isolation as a single enantiomer for possible applications in chirosciences. Studies on other cyclohelicenes and their applications are ongoing in our laboratories.

## *Acknowledgements*

Financial support from Aix Marseille University, Centrale Marseille, University of Bordeaux, Paris Saclay University, and the Centre National de la Recherche Scientifique (CNRS) is gratefully acknowledged. We thank Dr. L. Fischer (Univ. Bordeaux) and Dr. R. Oda (Univ. Bordeaux) for assistance with CPL spectroscopy.

## Conflict of interest

The authors declare no conflict of interest.

**Keywords:** aromatic compounds · chirality · chiroptical properties · conformation analysis · helical structures

[1] J. R. Grate Brandt, F. Salerno, M. J. Fuchter, *Nat. Chem. Rev.* **2017**, *1*, 0045.
[2] Reviews: a) M. Stępień, N. Sprutta, L. Latos-Grażyński, *Angew. Chem. Int. Ed.* **2011**, *50*, 4288–4340; *Angew. Chem.* **2011**, *123*, 4376–4430; b) M. Rickhaus, M. Mayor, M. Juríček, *Chem. Soc. Rev.* **2016**, *45*, 1542–1556; c) M. Rickhaus, M. Mayor, M. Juríček, *Chem. Soc. Rev.* **2017**, *46*, 1643–1660; d) M. A. Majewski, M. Stępień, *Angew. Chem. Int. Ed.* **2019**, *58*, 86–116; *Angew. Chem.* **2019**, *131*, 90–122. For recent examples: e) K. Senthilkumar, M. Kondratowicz, T. Lis, P. J. Chmielewski, J. Cybińska, J. L. Zafra, J. Casado, T. Vives, J. Crassous, L. Favereau, M. Stępień, *J. Am. Chem. Soc.* **2019**, *141*, 7421–7427; f) R. Kurosaki, M. Suzuki, H. Hayashi, M. Fujiki, N. Aratani, H. Yamada, *Chem. Commun.* **2019**, *55*, 9618–9621.
[3] a) B. Thulin, O. Wennerström, *Tetrahedron Lett.* **1977**, *18*, 929–930. For an alternative synthesis, see: b) D. N. Leach, J. A. Reiss, *J. Org. Chem.* **1978**, *43*, 2484–2487.
[4] H. Irngartinger, W. R. K. Reibel, G. M. Sheldrick, *Acta Crystallogr. Sect. B* **1981**, *37*, 1768–1771.
[5] T. V. V. Ramakrishna, P. R. Sharp, *Organometallics* **2004**, *23*, 3079–3081.

[6] Y. Zhen, W. Yue, Y. Li, W. Jiang, S. Di Motta, E. Di Donato, F. Negri, S. Ye, Z. Wang, *Chem. Commun.* **2010**, *46*, 6078 – 6080.
[7] a) W. Nakanishi, T. Matsuno, J. Ichikawa, H. Isobe, *Angew. Chem. Int. Ed.* **2011**, *50*, 6048 – 6051; *Angew. Chem.* **2011**, *123*, 6172 – 6175; b) T. Matsuno, K. Kogashi, S. Sato, H. Isobe, *Org. Lett.* **2017**, *19*, 6456 – 6459.
[8] a) B. Thulin, O. Wennerström, *Acta Chem. Scand. Sect. B* **1976**, *30*, 688 – 690; b) E. M. Kosower, H. Dodiuk, B. Thulin, O. Wennerström, *Acta Chem. Scand. Sect. B* **1977**, *31*, 526 – 528.
[9] a) A. Robert, P. Dechambenoit, E. A. Hillard, H. Bock, F. Durola, *Chem. Commun.* **2017**, *53*, 11540 – 11543; b) G. Naulet, L. Sturm, A. Robert, P. Dechambenoit, F. Röhricht, R. Herges, H. Bock, F. Durola, *Chem. Sci.* **2018**, *9*, 8930 – 8936.
[10] M. G. Belarmino Cabral, D. M. Pereira de Oliveira Santos, R. Cristiano, H. Gallardo, A. Bentaleb, E. A. Hillard, F. Durola, H. Bock, *ChemPlusChem* **2017**, *82*, 342 – 346.
[11] a) J. Courtieu, P. Lesot, A. Meddour, D. Merlet, C. Aroulanda in *Encyclopedia of NMR, Vol. 9* (Eds: D. M Grant, R. K. Harris), Wiley, Chichester, **2002**, pp. 497 – 505; b) P. Lesot, D. Merlet, M. Sarfati, J. Courtieu, H. Zimmermann, Z. Luz, *J. Am. Chem. Soc.* **2002**, *124*, 10071 – 10082; c) P. Lesot, C. Aroulanda, H. Zimmermann, Z. Luz, *Chem. Soc. Rev.* **2015**, *44*, 2330 – 2375.
[12] CCDC 1916096 for (*P*,*aR*,*P*,*aR*)-**3 b** and 1916097 for (*M*,*aS*,*M*,*aS*)-**3 b** contain the supplementary crystallographic data for this paper. These data are provided free of charge by The Cambridge Crystallographic Data Centre.
[13] R. Kuroda, *J. Chem. Soc. Perkin Trans. 2* **1982**, 789 – 794.
[14] G. Casalone, C. Mariani, A. Mugnoli, M. Simonetta, *Mol. Phys.* **1968**, *15*, 339 – 348.
[15] Y. Nakai, T. Mori, Y. Inoue, *J. Phys. Chem. A* **2012**, *116*, 7372 – 7385.
[16] a) E. M. Sánchez-Carnerero, A. R. Agarrabeitia, F. Moreno, B. L. Maroto, G. Muller, M. J. Ortiz, S. de la Moya, *Chem. Eur. J.* **2015**, *21*, 13488 – 13500; b) H. Tanaka, Y. Inoue, T. Mori, *ChemPhotoChem* **2018**, *2*, 386 – 402.
[17] J. Barroso, J. L. Cabellos, S. Pan, F. Murillo, X. Zarate, M. A. Fernandez-Herrera, G. Merino, *Chem. Commun.* **2018**, *54*, 188 – 191.
[18] Double [5]helicene: a) H. Kashihara, T. Asada, K. Kamikawa, *Chem. Eur. J.* **2015**, *21*, 6523 – 6527. Triple [5]helicenes: b) L. Barnett, D. M. Ho, K. K. Baldridge, R. A. Pascal Jr., *J. Am. Chem. Soc.* **1999**, *121*, 727 – 733; c) D. Peña, A. Cobas, D. Pérez, E. Guitian, L. Castedo, *Org. Lett.* **2000**, *2*, 1629 – 1632; d) H. Saito, A. Uchida, S. Watanabe, *J. Org. Chem.* **2017**, *82*, 5663 – 5668. Hextuple [5]helicenes: e) V. Berezhnaia, M. Roy, N. Vanthuyne, M. Villa, J.-V. Naubron, J. Rodriguez, Y. Coquerel, M. Gingras, *J. Am. Chem. Soc.* **2017**, *139*, 18508 – 18511; f) T. Hosokawa, Y. Takahashi, T. Matsushima, S. Watanabe, S. Kikkawa, I. Azumaya, A. Tsurusaki, K. Kamikawa, *J. Am. Chem. Soc.* **2017**, *139*, 18512 – 18521.

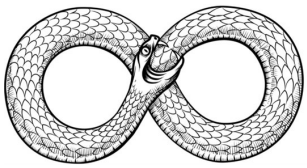

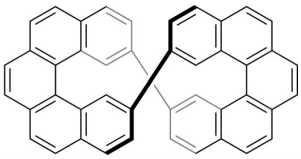

**The ouroboros**, a snake swallowing its own tail famous to chemists for its alleged role in the discovery of the structure of benzene by Kékulé, is sometimes represented as a lemniscate, a curve shaped like a figure-eight. At the molecular scale, cyclobishelicenes form a class of shape-persistent figure-eight aromatic molecules (see graphic), the conformational behavior and chirality-related properties of which are investigated for the first time.

**Helical Structures**

*A. Robert, G. Naulet, H. Bock, N. Vanthuyne, M. Jean, M. Giorgi, Y. Carissan, C. Aroulanda, A. Scalabre, E. Pouget, F. Durola,* Y. Coquerel**

■■ – ■■

**Cyclobishelicenes: Shape-Persistent Figure-Eight Aromatic Molecules with Promising Chiroptical Properties**